Atmos. Chem. Phys., 10, 8839–8854, 2010
www.atmos-chem-phys.net/10/8839/2010/
doi:10.5194/acp-10-8839-2010

Atmospheric Chemistry and Physics

Evaluation of a regional air quality forecast model for tropospheric NO_2 columns using the OMI/Aura satellite tropospheric NO_2 product

F. L. Herron-Thorpe, B. K. Lamb, G. H. Mount, and J. K. Vaughan

Laboratory for Atmospheric Research, Department of Civil & Environmental Engineering, Washington State University, Pullman, Washington, 99164-2910, USA

Received: 12 November 2009 – Published in Atmos. Chem. Phys. Discuss.: 15 December 2009
Revised: 24 August 2010 – Accepted: 26 August 2010 – Published: 20 September 2010

Abstract. Results from a regional air quality forecast model, AIRPACT-3, are compared to OMI tropospheric NO_2 integrated column densities for an 18 month period over the Pacific Northwest. AIRPACT column densities are well correlated ($r = 0.75$) to cloud-free (<35%) retrievals of tropospheric NO_2 for monthly averages without wildfires, but are poorly correlated ($r = 0.21$) with significant model overpredictions for months with wildfires when OMI and AIRPACT are compared over the entire domain. AIRPACT predicts higher NO_2 in some northwestern US urban areas, and lower NO_2 in the Vancouver, BC urban area, when compared to OMI. Model results are spatially averaged to the daily OMI swath. The Dutch KNMI (DOMINO) and NASA (Standard Product) retrievals of tropospheric NO_2 from OMI (Collection-3) are compared. The NASA product is shown to be significantly different than the KNMI tropospheric NO_2 product. The average difference in tropospheric columns, after applying the averaging kernels of the respective products to the model results, is shown to be larger in the summer (±50%) than winter (±20%).

1 Introduction

Nitrogen oxides (NO_x) are emitted into the atmosphere from natural sources, motor vehicles, and other combustion processes. NO_2, which causes adverse health effects, is regulated as an EPA criteria pollutant. NO_x acts as a chemical precursor to the formation of regional ozone, acid rain, and nitrate aerosol. NO_2 is an important component of urban atmospheric chemistry with large diurnal variations due to a strong dependence on mobile emissions and incident sunlight. In the past few decades, catalytic converters on automobiles have significantly reduced NO_x formation by catalytic reduction to O_2 and N_2. This has greatly reduced the emissions per vehicle, but regional ozone formation continues to be a problem. Studying regional air quality using Chemical Transport Models (CTMs) such as the Community Multi-scale Air Quality (CMAQ) model (Byun and Schere, 2006) can bring a greater understanding of atmospheric processes to scientists, policy makers, regulatory agencies, and the community. Continuous monitoring of air quality provides a framework for evaluating model results and increasing model accuracy. In the Pacific Northwest, the density of surface air-quality monitors is sparse, especially for measuring NO_x. NASA's Earth Observing Satellites (EOS) provide air-quality researchers with a rich resource of daily global observations of the atmosphere, including tropospheric NO_2 column densities. Despite limitations of EOS spatial and temporal resolution, as compared to a regional CTM, column retrievals may prove useful for evaluating NO_x emissions inventories.

State agencies and the US EPA collectively provide a detailed emissions inventory by source and type that can be used to drive CTMs. Emissions processing by the Sparse Matrix Operator Kernel Emissions (SMOKE) modeling system and its companion programs such as MOBILE6 (EPA, 2003) utilize meteorological inputs to produce emissions estimates with a high degree of variation in time and space. The lifetime of NO_x is short, so the presence of high values

Correspondence to: F. L. Herron-Thorpe (farrenthorpe@wsu.edu)

in the troposphere is indicative of daily emissions, and errors in a CTM's NO_x emission inventory should be evident when comparing satellite retrievals and model results for average daily NO_2. Emissions inventories for on-road vehicles have been particularly criticized (Parrish, 2006) and are difficult to predict given the variability of vehicle emissions. Recently, tropospheric NO_2 retrievals by satellite have been used to evaluate NO_x emission inventories used in CTMs through Kalman filter inversion (Napelenok, 2008). Assimilation through adjoint inverse modeling using 4d-var algorithms have also been developed as described in Kurokawa et al. (2009) and Elbern et al. (2007).

The OMI (Ozone Monitoring Instrument) is a Dutch instrument flying on the NASA Aura satellite launched in July 2004. OMI has excellent spatial resolution with pixels approximately 13 km×24 km at nadir in normal operational mode. Unique level-2 data products are created by both the KNMI (Royal Netherlands Meteorological Institute) and NASA science teams. These agencies employ different techniques for deducing tropospheric NO_2 column abundances; hence the retrieval results are not identical. Collection-3 tropospheric NO_2 is currently available to users from both KNMI and NASA. The KNMI website gives users access to near real-time (NRT) data of Europe and North America which are available within a few hours of the satellite overpass. This NRT data is valuable for applications needing access as quickly as possible (i.e. field studies), but is not guaranteed to have uninterrupted data delivery or be at the same quality as the official data collection. KNMI also provides online access to the averaging kernels and a priori profiles in VCD format, which are unique for each pixel.

1.1 Overall goals

For this analysis, we have chosen to use both the standard NASA and KNMI DOMINO (Derivation of OMI tropospheric NO_2) level-2 data products as sources of evaluation for the AIRPACT-3 regional air quality forecast system for tropospheric NO_2 over 18 months. The overall goals for this work are: 1) to establish a record of OMI retrievals of tropospheric nitrogen dioxide over the Pacific NW which includes the AIRPACT-3 spatial domain, 2) evaluate the AIRPACT-3 air quality forecast system by comparing to OMI NO_2 data, 3) improve our understanding of emissions and atmospheric chemistry in the Pacific Northwest by understanding the differences between the OMI data and the AIRPACT-3 model including application of the OMI averaging kernels to AIRPACT to achieve a rigorous tropospheric column comparison, and 4) share information about the OMI tropospheric nitrogen dioxide products that may be of use to other air quality scientists. Thus, the main objective of this paper is to examine the spatial and temporal distribution of NO_2 over the model domain by comparing OMI retrieval results to the AIRPACT-3 model results. We show that OMI air quality data products are useful for identifying large biases in AIRPACT-3 forecasts but are not certain enough to identify problems in low pollution areas.

1.2 AIRPACT-3: Air Indicator Report for Public Access and Community Tracking v.3

AIRPACT-3 is an air quality forecast system for the Pacific Northwest reporting to the public daily via the web. The AIRPACT system combines air chemistry and meteorology using community modeling software including the Weather Research Forecast (WRF) meteorological model (Mesoscale Model 5 (MM5) prior to April, 2008), the SMOKE processing system, and the Community Multi-scale Air Quality Model (CMAQ). WRF output fields are obtained from the University of Washington mesoscale meteorological forecast operations on a daily basis (http://www.atmos.washington.edu/mm5rt/, Mass et al., 2003). The WRF meteorological fields are processed using the MCIP program prior to use in CMAQ. Details about MCIP and the governing equations of CMAQ can be found in Byun and Schere (2006), which describes the calculations for advection, diffusion, chemical reactions, photolysis, cloud mixing, aerosol dynamics, and deposition. The AIRPACT-3 domain (shown in Fig. 1) uses 95×95 (9025 total) 12 km×12 km grid cells with 21 vertical layers increasing in layer thickness from the surface to the tropopause. Further details describing AIRPACT-3 and recent evaluation results are given in Chen et al. (2008). The forecast results, along with automated evaluation results based upon AIRNOW monitoring data, are provided on a daily basis on the AIRPACT web site (http://lar.wsu.edu/airpact-3).

The SMOKE tool is used to process anthropogenic emission categories for each forecast simulation. Area and non-road mobile emissions are based on the 2002 EPA NEI as adjusted using the EPA's Economic Growth Analysis System (EGAS) software. On-road mobile emissions are generated using emission factors from the EPA MOBILE v6.2 model and state specific activity data and are adjusted for WRF-forecast temperature. Anthropogenic emissions over the provinces of British Columbia and Alberta, Canada are included from the 2000 Greater Vancouver Regional District (GVRD) inventory. Fire emissions for the period of analysis were obtained from BlueSky (http://www.airfire.org/bluesky), utilizing ICS-209 reports and providing necessary inputs to SMOKE. More information about emissions processing in AIRPACT can be found in Chen et al. (2008).

1.3 OMI: Ozone Monitoring Instrument (http://aura.gsfc.nasa.gov/)

OMI makes daily retrievals of species such as NO_2, O_3, BrO, SO_2, and HCHO. The OMI Algorithm Theoretical Basis Document, Vol. 4 from NASA (Chance, 2002) discusses the specifics of trace gas retrievals, including NO_2. Aerosol optical density is also measured. Aura is in a

sun-synchronous orbit (overpass time ~01:45 p.m.) and flies in the "Afternoon-Train" (A-train) of satellites. The analysis in this paper utilizes the pixel level (level-2) OMI NO_2 (Collection-3) product where each orbital dataset is a 1644×60 grid, with $13\,km \times 24\,km$ footprint at nadir, and covers approximately 1/14th of the globe with varying area and angle during each orbit. Operational level-2 vertical column data from OMI is generally available within 1.5 days after the satellite overpass and NASA data can be obtained from the Mirador service provided by the NASA Goddard Space Flight Center (http://mirador.gsfc.nasa.gov); KNMI data is available from the Tropospheric Emission Monitoring Internet Service (TEMIS) at http://www.temis.nl/airpollution/no2.html. If users prefer data on a standard global grid, NASA offers this at 0.25 degree resolution.

The OMI NO_2 product is a useful data source for air-quality researchers because it provides a daily tropospheric NO_2 vertical column density at spatial resolutions useful for regional analyses. As discussed in Bucsela et al. (2006), the standard analysis of Earth spectral radiance measurements from OMI makes use of a radiative transfer model and a geo-referencing scheme to determine trace gas column abundances. In order to obtain the trace gas column abundances, use of a prior spatial distribution of both tropospheric and stratospheric NO_2 is required. Validation efforts for OMI NO_2, as discussed in Celarier et al. (2008) have shown that OMI is performing well and providing valuable data. For instance, during INTEX-B validation in Mexico (Boersma, 2008), a correlation of $r = 0.82$ and slope $= 0.99$ was found when OMI (NRT KNMI) was compared to airplane measurements. In the United Kingdom, the correlation was found to be between $r = 0.64$ and $r = 0.83$, depending on season (Kramer, 2008), when OMI was compared to MAX-DOAS ground measurements.

2 Methods

Use of trace gas columns from remote sensing instruments on polar orbiting satellite instruments involves a number of limitations when comparing to the AIRPACT tropospheric air quality model. These include: 1) cloud cover that limits the depth of the retrieval as seen from space, 2) only one useful day-time data value is reliably obtained per geo-location, 3) horizontal resolution is coarser than the model, and 4) the conversion of observed slant columns to useful tropospheric column abundances is difficult. The standard cloud-screened tropospheric NO_2 product from OMI (level-2G) uses pixels with cloud fraction less than 30% (Celarier, 2009), while some studies use pixels with cloud fraction up to 40% (Mijling, 2009) when there are limited cloud-free days. Using a 30% limit on cloud fraction for the Pacific Northwest significantly limits available pixels, due to frequent cloud cover. However, using OMI pixels with cloud fraction less than 40% significantly changes the calculated monthly average values because of the large "below cloud" additions associated with using the additional pixels. For these reasons, our analysis only uses tropospheric NO_2 pixels with less than 35% cloud cover. Afternoon data from AIRPACT and OMI were matched and averaged by month for comparison. These monthly averages are analyzed for the entire domain with a focus on biases in urban areas and some attention given to wildfire periods/locations. To properly evaluate the linear correlation (Pearson's r) between OMI and AIRPACT VCD monthly average spatial distributions, we spatially averaged the AIRPACT grid to the pixels within the daily OMI swaths. We also tested the effects of applying the OMI averaging kernel to the AIRPACT data to account for assumptions made in the OMI retrieval and allow a consistent comparison between the modeled and measured columns.

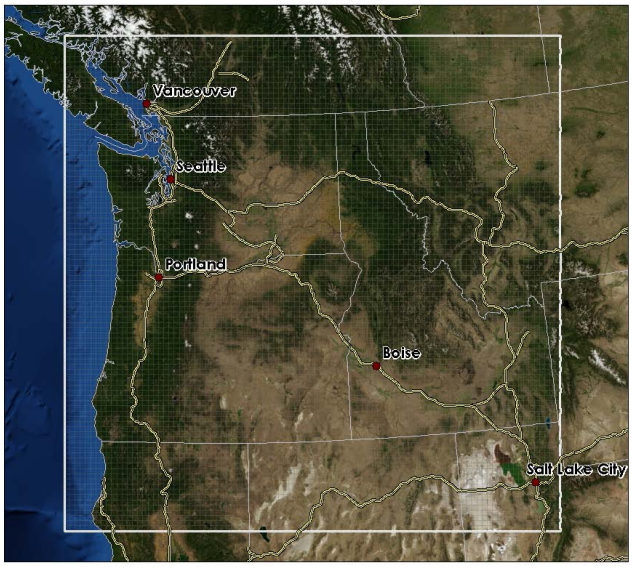

Fig. 1. The AIRPACT-3 domain Satellite imagery of the AIRPACT-3 domain is shown with interstate freeways as yellow lines and large cities as red dots.

The work presented here is an analysis of 18 months, from March 2007 to August 2008, that compares OMI and AIRPACT tropospheric NO_2 columns within the AIRPACT domain.

2.1 Independent AIRPACT column derivation

For the period of analysis presented here, daily AIRPACT forecasts provide hourly averages of trace gases as mixing ratios which are converted to a "vertical column density" for and summed vertically for direct comparison to tropospheric column density satellite retrievals. A layer's vertical column density (VCD) can be calculated from:

$$\mathrm{VCD} = \frac{m_R\ (\mathrm{ppm})}{10^6} \cdot L_T\ (\mathrm{cm}) \cdot n_0\ (\mathrm{molecules/cm^3}) \qquad (1)$$

where m_R is the mixing ratio of the trace gas, L_T is the model layer thickness, and n_0 is the number of total gas molecules per volume (Loschmidt's number). Loschmidt's number is dependent on temperature, pressure, and the gas constant:

$$n_0 = \frac{P}{R \cdot T} \tag{2}$$

Substituting in the definition of n_0 and summing across all 21 layers yields:

$$\mathrm{VCD} = \sum_{i=1}^{21} \frac{m_{Ri}}{10^6} \cdot \frac{L_{T_i} \cdot P_i \cdot N_A}{R \cdot T_i} \tag{3}$$

Accounting for units, and adjusting for available parameters from the MCIP GRIDCRO3D and CMAQ CONC files, we finally get:

$$\mathrm{VCD} = \sum_{i=1}^{21} m_{Ri} \cdot \frac{2 \cdot (\mathrm{ZF}_i - \mathrm{ZH}_i) \cdot \mathrm{PRES}_i}{\mathrm{TA}_i} \cdot 7.243 \cdot 10^{12} \tag{4}$$

where VCD is the vertical column density in molecules/cm^2, ZF is the layer full height in meters, ZH is the layer half height in meters, PRES is the layer pressure in pascals, and TA is the layer temperature average in Kelvins. MCIP does not report layer thickness, so L_T has been replaced with twice the difference of the layer's full and half height. This derivation of VCD from CMAQ and MCIP variables is independent of trace gas species.

2.2 OMI tropospheric NO_2 column

NO_2 is found in both the troposphere and stratosphere and so the total columns retrieved from OMI include contributions from both regions of the atmosphere. In KNMI's DOMINO product, the contribution of stratospheric NO_2 is deduced from a chemistry-transport model and subtracted from the retrieved total column, resulting in a tropospheric column density. This method is based on previous SCIAMACHY/GOME retrieval algorithms and described further in Dirksen et al. (2008). The tropospheric NO_2 algorithm used in NASA's standard product is based on derivations of "polluted" and "unpolluted" portions of the column with the tropospheric column calculated as 5% of the unpolluted portion plus the entire polluted portion in polluted areas and calculated as 5% of the total column when no polluted portion is derived. This method is described further in the OMINO2 README File (2009).

OMI level-2 algorithms calculate a tropospheric NO_2 VCD for each OMI pixel. Below cloud NO_2 in the NASA product, called the "ghost column" in the KNMI product, is estimated from the a priori profile shape of the pixel and OMI's measurement of NO_2 above the cloud cover pressure level and is described further in the OMNO2 README File (2009). Summing the below cloud and tropospheric NO_2 gives the user a representation of a full column of NO_2 in the troposphere above the ground. However, the below cloud NO_2 addition is not based on any observation below the clouds. To account for this, our monthly average calculations are limited to using pixels with less than a 35% cloud fraction reported by OMI, with corresponding daily values from AIRPACT masked from averaging.

The tropospheric columns that are calculated rely on meteorological variables that affect the number density of molecules throughout the atmosphere. This is quite simple for a model, as all variables can be exported and the user has a complete "state" of the atmosphere. However, NASA's OMI algorithms use global model results for the average temperature and pressure on a coarse grid, and do not use current meteorological observations (or recent forecasts) to determine a layer's temperature or pressure. Using the ideal gas law, simple calculations of variance in number density due to a few degrees of temperature or tens of millibars suggest this error is small. However, significant retrieval errors may occur when the surface pressure used is not accurate, especially over regions with complex topography as discussed by Boersma (2007). In contrast, KNMI's DOMINO product assimilates realistic meteorological fields from the European Centre of Medium-Range Forecasts (ECMWF) to drive the CTM used to derive a priori profiles (Dirksen, 2008).

The a priori NO_2 fractional abundances used by KNMI algorithms are generated from daily global Tracer Model version 4 TM4 results (Fig. 2) which are used to calculate the OMI AMF and "ghost column" NO_2 (Mijling, 2007). The TM4 model results have a 2° latitude × 3° longitude horizontal resolution and are interpolated spatially and temporally to provide input for the level-2 product. The a priori NO_2 profiles used by the NASA algorithms to calculate the AMF and below cloud NO_2 are separated into "polluted" (lower tropospheric) and "unpolluted" (stratospheric and a small amount of upper tropospheric) profiles and are generated from annually averaged global GEOS-CHEM results (Bucsela, et al, 2006) (e.g., Fig. 3) . The GEOS-CHEM results have a $2^\circ \times 2.5^\circ$ horizontal resolution and are re-gridded by NASA to $2^\circ \times 2^\circ$ for use in the OMI algorithms using a nearest neighbor approach.

2.3 Accounting for varied resolution

The OMI level-2 products provide many different variables such as viewing and sun geometry, cloud properties, pressures, reflectivity, radiances, and retrieved columns which vary per OMI pixel. Furthermore, each OMI pixel has a different location, size, and orientation. In order to properly compare the static model grid to the varying satellite grid, the AIRPACT cells that fall within the spatial boundaries of each OMI pixel must be averaged and interpolated, effectively reducing the resolution of the model results to equal that of the co-located OMI pixel.

After AIRPACT values were spatially averaged to the OMI pixels, we interpolated the OMI and AIRPACT grids to a Lambert equal area projection with a horizontal resolution

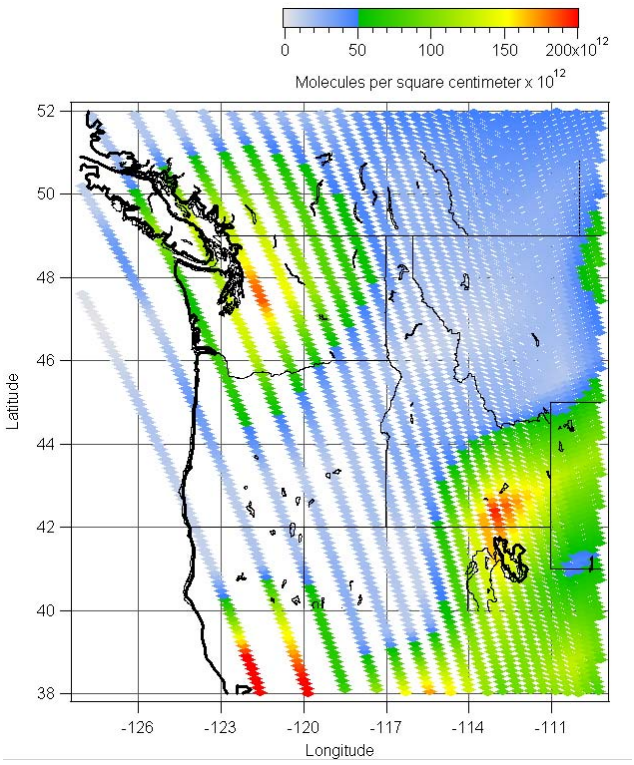

Fig. 2. A sample a priori map of surface layer NO_2 used in DOMINO algorithms, developed with global TM4 simulations at a $3° \times 2°$ resolution, plotted as OMI pixel centers for one swath (3 July 2007 shown). This data is provided daily by KNMI, interpolated to the daily OMI swath.

equal to that of AIRPACT, through use of a Delaunay triangulation scheme. Once the data were on a common grid, scripting was used to perform the calculation of domain biases, averages, and urban area timelines for all comparisons over the 18 month period.

2.4 The OMI tropospheric NO_2 averaging kernel

An averaging kernel expresses the relative sensitivity of an instrument to the abundance of the target species within the layers throughout the atmospheric column. When comparing AIRPACT model results with trace gas satellite retrievals, an instrument averaging kernel should be applied to the modeled layers so the derived column can be more correctly compared to the observations (Bucsela, 2008). This then accounts in the modeled data for meteorological assumptions made when calculating the OMI air mass factor as well as geometry, terrain variables, cloud properties, and a modeled a priori NO_2 profile for each observation. This approach can be numerically intensive because it requires many more variables and functions, than does a simple summed tropospheric column comparison. Application of the averaging kernel is particularly important for nadir looking solar backscatter instruments, such as OMI, because those measurements show their least sensitivity to the atmosphere near the Earth's surface.

The averaging kernel of a total column (A) is a unitless vector mapped to the a priori vertical layers. Values less than one are typically calculated for the boundary layer and greater than one for the free troposphere and stratosphere. For comparison to tropospheric column satellite retrievals, the tropospheric averaging kernel (A_{trop}),

$$A_{\text{trop}} = A \cdot \frac{\text{AMF}}{\text{AMF}_{\text{trop}}} \tag{5}$$

is applied to the vertical vectors of modeled NO_2 (x_{trop}) to obtain the desired column (y_{trop}):

$$y_{\text{trop}} = A_{\text{trop}} \cdot x_{\text{trop}} \tag{6}$$

where AMF is the air mass factor for total columns and AMF_{trop} corresponds to the tropospheric air mass factor. This method requires vertical interpolation of the data to the pressure levels of the a priori profiles used in the algorithms, or interpolation of the averaging kernel profiles to the user pressure levels (Boersma et al., 2009). The averaging kernels and all related variables are included in the level-2 KNMI data product available to all users (http://www.temis.nl/airpollution/no2col/no2regioomi_col3.php). The NASA data product does not include any averaging kernels, so programs and annual GEOS-CHEM lookup tables (E. J. Bucsela, personal communication, 2008) were obtained to compute the NASA averaging kernel for each OMI pixel.

3 Results and discussion

Our analysis focuses on four areas: 1) the effects of spatial averaging, 2) long term biases in the AIRPACT forecast results that were observed when compared to both OMI KNMI and NASA tropospheric NO_2 retrievals, 3) long term differences between the KNMI and NASA tropospheric NO_2 retrievals, and 4) the effect of applying KNMI and NASA averaging kernels to the AIRPACT results. Table 1 summarizes the different variations of datasets analyzed in this section.

3.1 Spatial averaging

In general, spatial averaging decreases steep trace gas abundance gradients near high concentration locations (e.g. city centers) and smoothes out minima and maxima. The degree of the smoothing is directly related to the size of the OMI pixels which are coarser than the AIRPACT grid. Thus, spatially averaging AIRPACT values to OMI pixel size before comparing to OMI is important. Independent AIRPACT tropospheric columns of NO_2 (a) and AIRPACT results spatially averaged to the OMI swath (b) are shown in Figs. 4 and 5 for two different monthly averages.

Table 1. The tropospheric NO_2 columns analyzed and the variables used for VCD.

Data Source	VCD Integration
1. OMI Retrieved Radiances	
KNMI	VCD = Tropospheric Column + Ghost Column
NASA	VCD = Tropopsheric Column + Below Cloud
2. AIRPACT Model Results	
AIRPACT	VCD(Pres., Temp., Height, Mixing Ratio)
SA-AIRPACT	VCD(Pres., Temp., Height, Mixing Ratio)
SA-AIRPACT	VCD(Pres., Mixing Ratio)*
SA-AIRPACT × DAK	VCD(Pres., Temp., Height, Mixing Ratio)
SA-AIRPACT × NAK	VCD(Pres., Temp., Height, Mixing Ratio)
SA-AIRPACT × NAK	VCD(Pres., Mixing Ratio)*

* Integration method similar to that used in NASA tropospheric algorithm (Provided by Bucsela) This method is discussed but not used in the overall analysis.
DAK = Domino Averaging Kernel.
NAK = NASA Averaging Kernel.
SA = Spatially Averaged to the daily OMI swath.

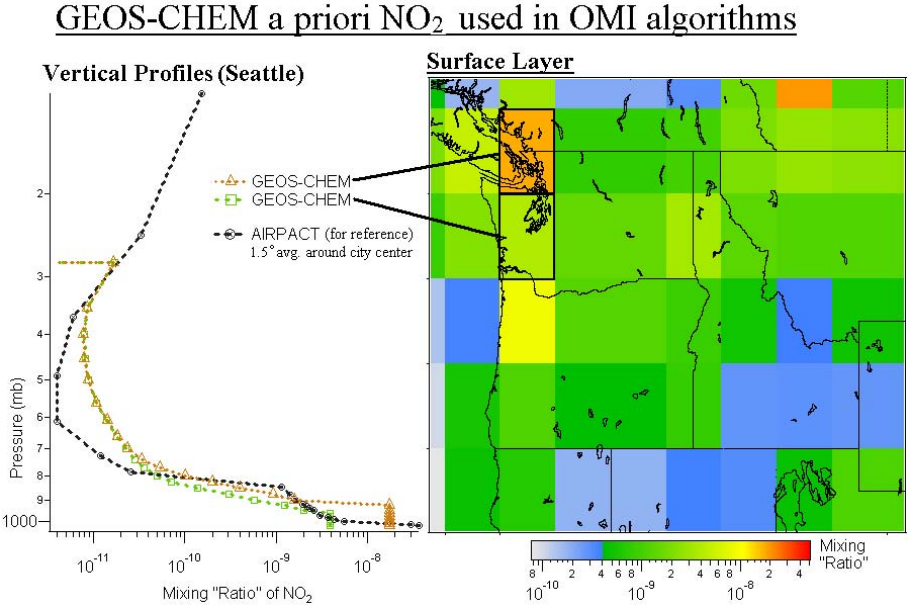

Fig. 3. A priori NO_2 used in OMI NASA algorithms, developed by Randall Martin with GEOS-CHEM simulations. The grid below is a $2^\circ \times 2^\circ$ matrix used for the OMI (NASA) algorithm, regridded from the original GEOS-CHEM simulations with original resolution of $2^\circ \times 2.5^\circ$. Note the profiles shown for two pixels over the Seattle metro area; these profiles show nearly an order of magnitude difference at the surface layer.

3.2 General differences between AIRPACT-3 and OMI tropospheric NO_2

In this section we discuss an 18-month analysis of OMI and AIRPACT tropospheric NO_2 which shows areas where AIRPACT demonstrates a significant bias relative to both the NASA and KNMI OMI L2 retrievals, without applying the OMI averaging kernels to AIRPACT. For example, AIRPACT predicts higher values in Seattle and lower values in Vancouver, BC during the summer. Correlations over the entire domain and general biases in specific areas are summarized on a monthly basis in Table 2. Overall, AIRPACT is better correlated to NASA retrievals than to KNMI retrievals. However, current AIRPACT predictions of NO_2 due to emissions from summer wild fires are considerably higher than retrievals by OMI (as are AIRPACT's CO fire emissions as compared to retrievals by AIRS – not shown). It is evident that the correlation is drastically reduced during summer

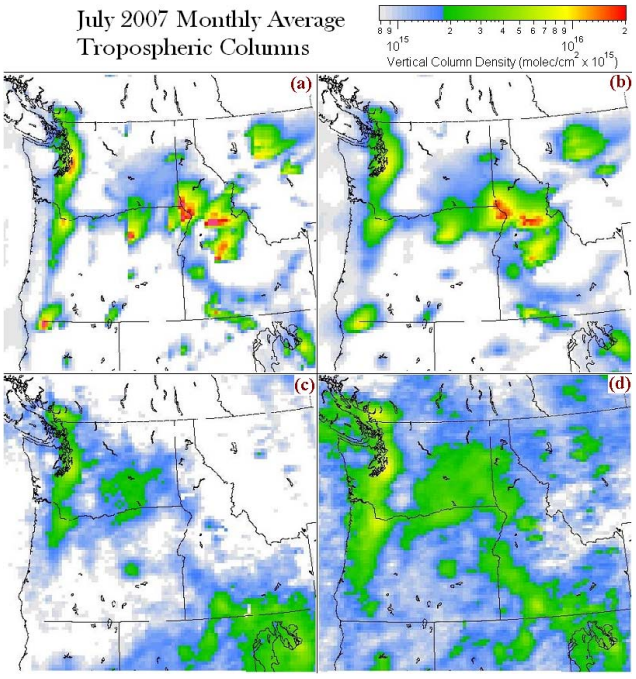

Fig. 4. Average tropospheric NO_2 columns are shown for the month of July, 2007: AIRPACT **(a)** at upper left, spatially averaged AIRPACT **(b)** at upper right, KNMI OMI **(c)** at lower left, and NASA OMI **(d)** at lower right.

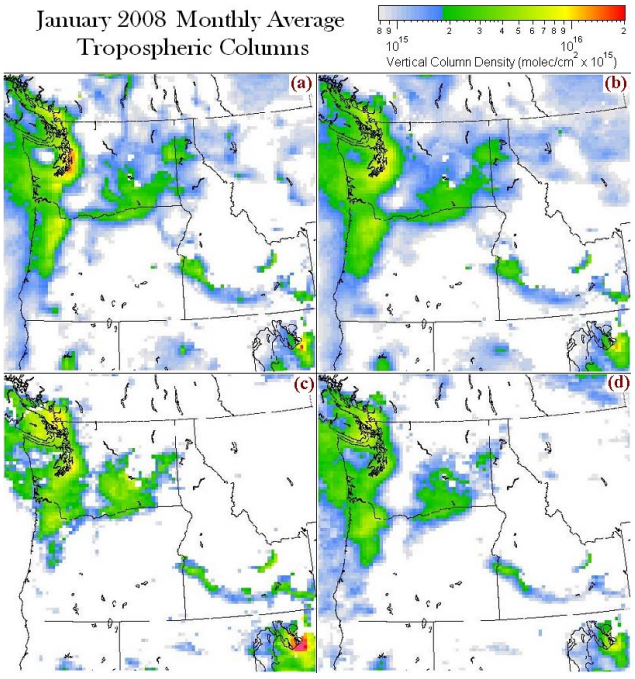

Fig. 5. Average tropospheric NO_2 columns are shown for the month of January, 2008: AIRPACT **(a)** at upper left, spatially averaged AIRPACT **(b)** at upper right, KNMI OMI **(c)** at lower left, and NASA OMI **(d)** at lower right. The pink color denotes values over 2×10^{16} molecules per square centimeter.

months where wildfires influence emissions in the domain. This strongly suggests that current emission factors for NO_2 from wildfires may be overestimated and/or that the fire size and progression in the BlueSky analyses used here is incorrect. Figure 4 shows the many fire hot spots that AIRPACT forecasted with high NO_2 emissions during summer wildfires of July 2007. Notice the fires in South Oregon, Central Idaho, and Montana. For comparison, Fig. 5 shows January 2008, when there were no recorded wildfires and emissions are largely from anthropogenic sources. Temporally averaged tropospheric column NO_2 densities in wildfire areas display very large discrepancies, as large as an order of magnitude. Increased smoke/cloud cover could result in OMI being unable to get a reliable measurement of boundary layer NO_2 in fire areas. OMI does, however, consistently retrieve large NO_2 signatures in areas of active wildfires. This may be attributed to the way fire size and progression were estimated in BlueSky which relied only on ICS-209 ground reports; more recent versions of the BlueSky framework merge these reports with satellite detects to produce a more reliable estimate of fire size and progression. Further work is required to see if these changes will improve the comparison between AIRPACT and OMI in the vicinity of wildfires.

Boersma (2008) determined top-down surface NO_x emissions for March 2006 over the contiguous United States and Mexico from NRT OMI data. The results were compared to bottom-up inventories for the INTEX-B domain by the US and Mexico Environmental Protection Agencies (US: 1999 National Emission Inventory (NEI99)). Modeled emissions of NO_x were shown to be too high in the United States while Mexican emissions were too low. The analysis showed that for the US EPA NEI99 inventory point source NO_x emissions should be lowered and mobile emissions increased to get agreement with OMI observations.

For our analyses, the 18 monthly averages for all three data sources and their spatial variations are graphed for 5 major urban areas: Portland, Oregon (Fig. 6); Boise, Idaho (Fig. 7); Vancouver, BC (Fig. 8); Salt Lake City, Utah (Fig. 9); and Seattle, Washington (Fig. 10). Generally, AIRPACT is between the range of NASA and KNMI retrievals in Salt Lake City, Boise, and Portland. However, AIRPACT forecasts of Seattle NO_2 columns are generally higher than OMI retrievals. Our results with AIRPACT, though largely based on EPA's 2002 NEI, bring us to conclusions similar to Boersma (2008) regarding the biases of NO_x emissions inventories used in urban areas when comparing Canada and the United States. Vancouver, BC shows very good correlation between AIRPACT and both OMI products for many months, but AIRPACT is clearly below the two OMI products for multiple months. This discrepancy could be due to a different emissions scenario from Canadian inventories.

Table 2. Linear correlation and best fit slope of AIRPACT-3 to OMI tropospheric NO_2 column monthly averages for the entire domain. Corresponding areas where both KNMI and NASA showed the same relative bias to AIRPACT are noted.

		AIRPACT to KNMI slope	r	AIRPACT to NASA slope	r	Corresponding Biases
2007	MARCH	0.36	0.593	0.98	0.715	Higher AIRPACT values in I-5 Corridor from Portland to Seattle. Higher OMI values in Victoria and surrounding Vancouver.
2007	APRIL	0.52	0.636	0.81	0.769	Higher AIRPACT values in Seattle. Higher OMI values in Victoria and Vancouver.
2007	MAY	0.72	0.715	0.80	0.728	Higher AIRPACT values in I-5 corridor from Portland to Seattle. Higher OMI values in Salt Lake, Victoria, and Vancouver
2007	JUNE	0.78	0.682	0.83	0.806	Higher AIRPACT values in Seattle and Portland. Higher OMI values in Salt Lake, Victoria, Vancouver, and central Washington.
2007	JULY	0.32	0.190	0.74	0.406	Much higher AIRPACT values in fire areas & higher values in Seattle. Higher OMI values in Vancouver, Salt Lake, north NV, and south ID.
2007	AUGUST	1.74	0.120	1.87	0.214	Much higher AIRPACT values in fire areas. Higher OMI values in Vancouver and Salt Lake.
2007	SEPTEMBER	−0.50	−0.066	0.00	0.000	Much higher AIRPACT values in fire areas. Higher OMI values in Vancouver and central Washington
2007	OCTOBER	0.10	0.047	0.31	0.113	Much higher AIRPACT values in fire areas. Higher AIRPACT values in Seattle. Higher OMI values in Vancouver.
2007	NOVEMBER	0.38	0.671	0.99	0.834	Higher AIRPACT values in Seattle and Boise. Higher OMI values in Vancouver
2007	DECEMBER	0.19	0.380	0.66	0.729	Higher AIRPACT values over Washington, Montana, and Idaho. Higher OMI values in greater Calgary and Vancouver.
2008	JANUARY	0.31	0.626	0.92	0.840	Higher AIRPACT values in Washington and Portland. Higher OMI values in Victoria.
2008	FEBRUARY	0.35	0.680	1.10	0.868	Higher AIRPACT values in the Rockies, especially Boise and Spokane. Higher OMI values in Canadian waters.
2008	MARCH	0.39	0.619	0.68	0.678	Higher AIRPACT values in Seattle. Higher OMI values in Victoria, Vancouver, & Tri-Cities
2008	APRIL	0.68	0.715	0.68	0.735	Higher AIRPACT values in Seattle. Higher OMI values in central Washington, Victoria, and Vancouver.
2008	MAY	0.86	0.672	0.74	0.574	Higher AIRPACT values in I-5 Corridor from Portland to Seattle. Higher OMI values in Victoria and central Washington.
2008	JUNE	1.01	0.727	0.90	0.747	Higher AIRPACT values in Seattle & Portland. Higher OMI values in Victoria and Vancouver.
2008	JULY	2.16	0.277	1.82	0.306	Much higher AIRPACT values over fires. Higher AIRPACT values in Seattle and Portland. Higher OMI values in Vancouver.
2008	AUGUST	1.06	0.191	0.71	0.191	Much higher AIRPACT values over CA fires. Higher AIRPACT values in Seattle. Higher OMI values in Salt Lake and ID/NV/UT fire.

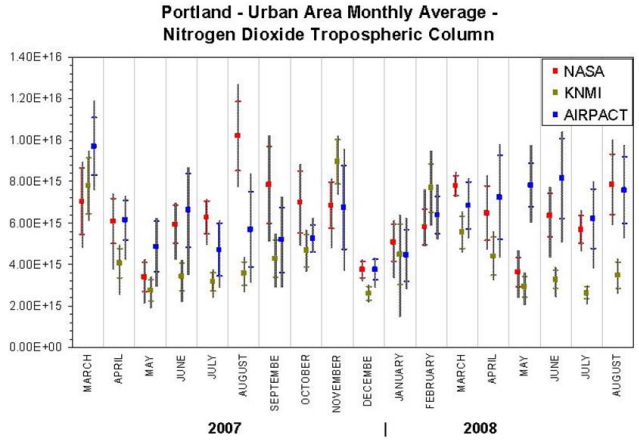

Fig. 6. Monthly Average NO_2 for Portland, Oregon over 18 months. The bars show standard deviation of spatial variation over a 1152 km^2 area (8 AIRPACT pixels) while the whiskers show the extent of the maximum and minimum. Values are in molecules per square centimeter.

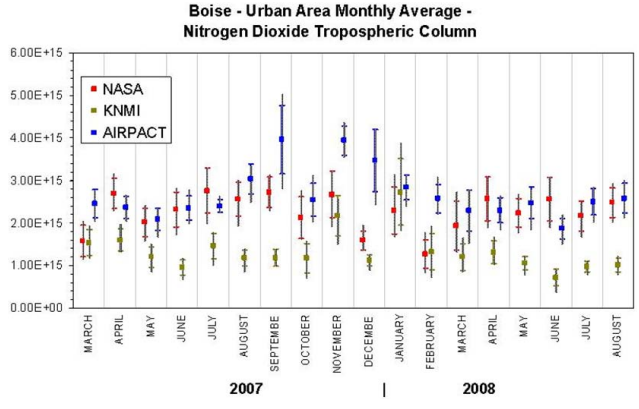

Fig. 7. Monthly Average NO_2 for Boise, Idaho over 18 months. The bars show standard deviation of spatial variation over a 720 km^2 area (5 AIRPACT pixels) while the whiskers show the extent of the maximum and minimum. Values are in molecules per square centimeter.

3.3 Differences in NASA and KNMI datasets

For the 18-month period of March 2007 to August 2008, an average correlation of $r = 0.68$ was calculated between the two OMI tropospheric NO_2 monthly averaged datasets. Generally the correlation was between 0.65 and 0.75, but two months had correlation below 0.5 because of the strong contribution of negative column values from KNMI. In fact, the KNMI datasets include negative values which can significantly dominate some pixels when calculating a monthly average, especially after masking clouded pixels. KNMI negatives are a result of subtracting too large of a stratospheric NO_2 contribution from the column; note that the NASA algorithm does not produce negative values, as it does not "subtract" the stratosphere. Table 3 shows the month-to-month correlation of KNMI to NASA datasets over the entire AIRPACT domain with commentary on general biases.

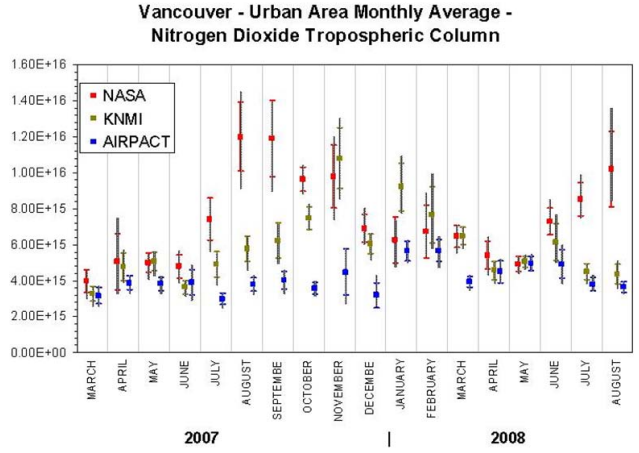

Fig. 8. Monthly Average NO_2 for Vancouver, British Columbia over 18 months. The bars show standard deviation of spatial variation over a 720 km^2 area (5 AIRPACT pixels) while the whiskers show the extent of the maximum and minimum. Values are in molecules per square centimeter.

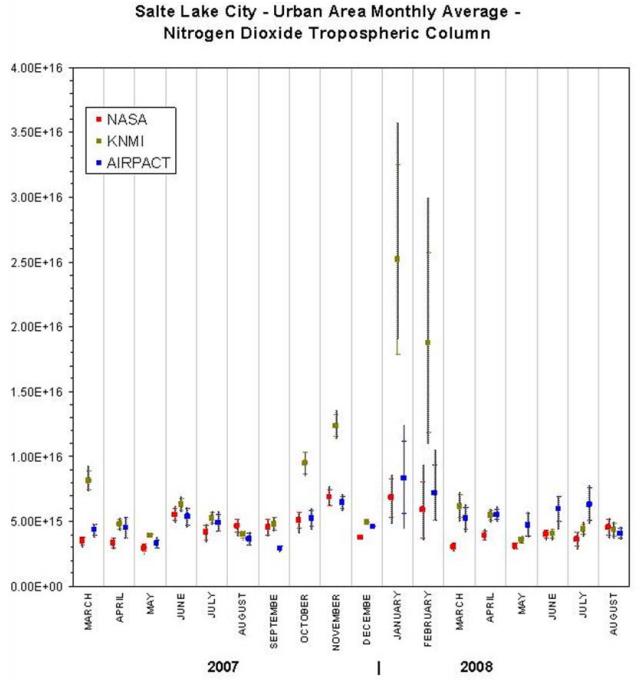

Fig. 9. Monthly Average NO_2 for Salt Lake City, Utah over 18 months. The bars show standard deviation of spatial variation over a 720 km^2 area (5 AIRPACT pixels) while the whiskers show the extent of the maximum and minimum. Values are in molecules per square centimeter.

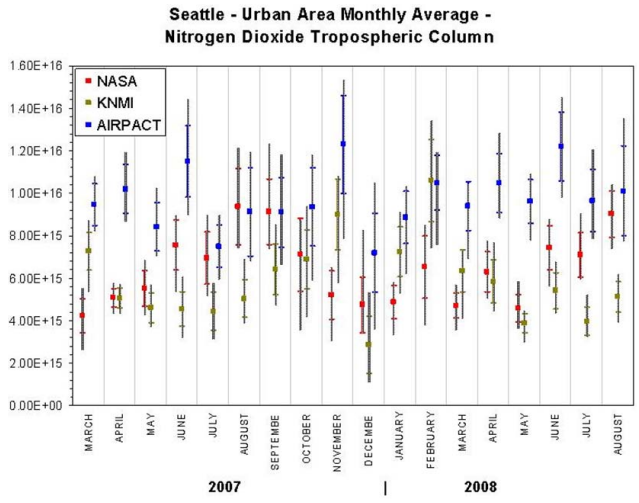

Fig. 10. Monthly Average NO_2 for Seattle, Washington over 18 months. The bars show standard deviation of spatial variation over a 1728 km^2 area (12 AIRPACT pixels) while the whiskers show the extent of the maximum and minimum. Values are in molecules per square centimeter.

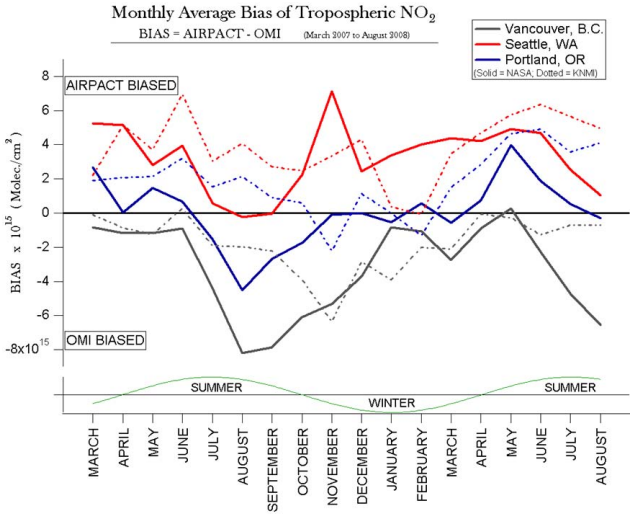

Fig. 11. Monthly average AIRPACT (spatially averaged) minus OMI, tropospheric NO_2 column biases in urban areas along the Interstate-5 Freeway from March 2007 to August 2008. Solid lines show NASA bias and dotted lines show KNMI bias. See Figs. 6, 8 and 10 for corresponding total tropospheric columns.

Tropospheric NO_2 columns calculated by NASA are lower during the winter (Fig. 5d) and higher during the summer (Fig. 4d) due to the way that the tropospheric column is calculated in the OMI NO_2 algorithms. This annual cyclic variance in tropospheric NO_2 found in the NASA product (Fig. 11) is not real, but rather an artifact of the known issues with the NASA OMI NO_2 algorithms. The main reason this seasonal artifact occurs is because annual a priori NO_2 profiles from GEOS-CHEM are used in the algorithms, rather than monthly profiles. E. J. Bucsela (personal communication, 2008), has identified two other issues that may cause smaller anomalies in the tropospheric product: 1) the small amounts of tropospheric contamination in the data used to derive the stratosphere and 2) issues introduced in the wave-2 interpolation. Wave-2 interpolation issues include the shapes of continents in the masked regions and the potential to hide planetary-scale structure in the troposphere (e.g. from lightning NO_x) and small-scale structure in the stratosphere. Stratospheric NO_2 is highest in the mid-latitudes during the summer (Cohen et al., 2003) and NASA's tropospheric NO_2 algorithms do not seem to account enough for the stratospheric contributionto the "unpolluted" columns for summer months.

The KNMI/TEMIS tropospheric NO_2 datasets do not show as much of a clear seasonal variation that the NASA datasets do. This is probably due to the fact that KNMI does not use annual a priori NO_2 profiles. DOMINO algorithms also capture small scale structures in the stratosphere not picked up by NASA's wave-2 interpolation (E. J. Bucsela, personal communication, 2010). There is still a small seasonal variation in unpolluted tropospheric NO_2 columns

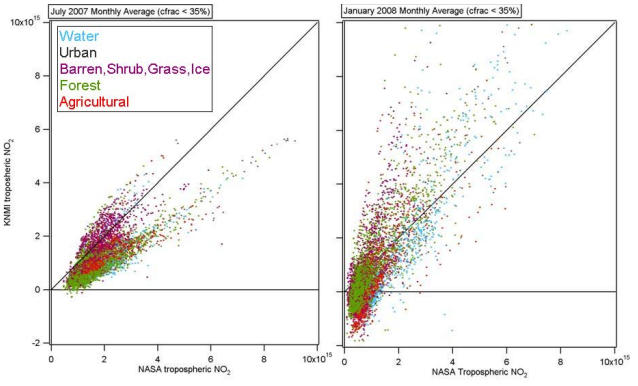

Fig. 12. KNMI vs. NASA tropospheric NO_2 from OMI for summer (July 2007 at left) and winter (January 2008 at right) monthly averages in molecules per square centimeter. Color denotes dominant land class type within the cell. Ideally a user may expect the distribution to fall roughly along the 1 to 1 line, if the two OMI products agreed well.

in the KNMI product, as more negatives are created in the winter, shown in Fig. 12. However, this does not seem to affect polluted areas.

Overall, the differences between the NASA and KNMI tropospheric NO_2 products are quite significant despite being derived from the same level-1 radiances. This difference makes it difficult for users to decide which data set to use for comparison. Figure 12 clearly shows that the NASA product reports the majority of values in winter between 0 and 1×10^{15} molecules per square centimeter while KNMI reports many values as less than zero. KNMI also reports

Table 3. Linear correlation and best fit slope of KNMI to NASA OMI tropospheric NO_2 column monthly averages for the analyzed domain. General biases are noted.

		KNMI to NASA slope	*r*	General Biases Comments
2007	MARCH	1.41	0.627	Higher NASA values over coastal waters. Higher KNMI values in Salt Lake and I-5 corridor from Portland to Seattle.
2007	APRIL	0.91	0.704	Higher NASA values over I-5 in Oregon, Spokane, and Boise. Higher KNMI values in western Washington and Salt Lake.
2007	MAY	0.83	0.758	Higher NASA values or no bias over most of the domain.
2007	JUNE	0.68	0.755	Higher NASA values over most of the domain. Higher KNMI values in the Cascades and Salt Lake.
2007	JULY	0.65	0.601	Higher NASA values over most urban areas in the domain. Higher KNMI values in Salt Lake.
2007	AUGUST	0.46	0.773	Higher NASA values or no bias over the entire domain.
2007	SEPTEMBER	0.57	0.794	Higher NASA values or no bias over the entire domain.
2007	OCTOBER	0.61	0.476	Higher NASA values over northern part of domain. Higher KNMI values in Salt Lake and central Washington.
2007	NOVEMBER	1.50	0.725	Higher KNMI values in Salt Lake, Washington, Vancouver, and Victoria. Higher NASA values in BC, Idaho, and Montana.
2007	DECEMBER	0.63	0.348	Higher NASA values over coastal waters, western Oregon, Vancouver, Victoria, and the Rockies. Higher KNMI values surrounding Salt Lake.
2008	JANUARY	1.52	0.690	Higher NASA values over coastal waters, Portland, and the Rockies. Higher KNMI values over Salt Lake, Washington I-5, Victoria, and Vancouver
2008	FEBRUARY	1.70	0.721	Higher KNMI values in Salt Lake, western Washington, and western BC.
2008	MARCH	0.91	0.582	Higher NASA values over water and I-5 in Oregon. Higher KNMI values in Salt Lake, west Washington, and Victoria.
2008	APRIL	0.71	0.733	Higher NASA values over water, Western Oregon, Eastern Washington, and Boise. Higher KNMI values in Salt Lake.
2008	MAY	0.69	0.688	Higher NASA values over most of the domain. Higher KNMI values in the Cascades.
2008	JUNE	0.68	0.780	Higher NASA values over most of the domain.
2008	JULY	0.50	0.661	Higher NASA values over most of the domain. Higher KNMI values in Salt Lake.
2008	AUGUST	0.49	0.728	Higher NASA values or no bias over the entire domain.

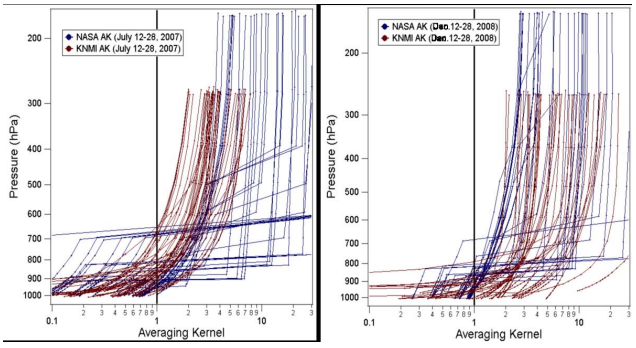

Fig. 13. A comparison of OMI tropospheric NO_2 averaging kernel profiles for Seattle, applied to the AIRPACT results for July 2007 (left) and January 2008 (right). The NASA averaging kernels were output explicitly from Bucsela's code using AIRPACT pressure layers while the KNMI kernels were converted to the AIRPACT pressure layers using a cubic-spline interpolation at 2 hPa spacing. The vertical extent of the KNMI averaging kernel is one layer less than that derived from Bucsela's code. The top tropospheric layer of NO_2 in the model is multiple orders of magnitude less in molecular abundance than the surface layers, so the contribution is insignificant to the total tropospheric column. However, it is the portion in the profile with the most instrument sensitivity, which results in the largest averaging kernel value.

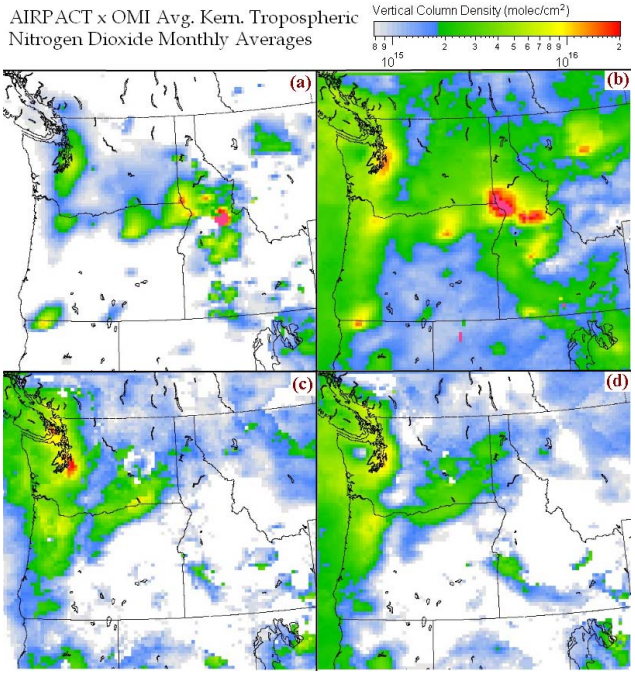

Fig. 14. Tropospheric NO_2 columns with the daily averaging kernels from OMI applied to AIRPACT are shown for summer (July, 2007) and winter (January 2008) monthly averages: AIRPACT × KNMI AK for July 2007 **(a)** at upper left, AIRPACT × NASA AK for July 2007 **(b)** at upper right, AIRPACT × KNMI AK for January 2008 **(ac)** at lower left, and AIRPACT × NASA AK for January 2008 **(d)** at lower right. The pink color denotes values over 2 × 10^{16} molecules per square centimeter.

much higher values than NASA over select urban areas during the winter. AIRPACT will not predict negative column abundances, so correlation with KNMI datasets will usually be slightly lower than NASA. Small column abundances in unpolluted areas should be compared with caution but large polluted areas have more comparable columns. KNMI values for urban areas are larger during winter months, especially Salt Lake City. Portland values are quite small during summer months, which is in contrast to the NASA product. Also, KNMI values over Vancouver are largest in the fall and winter as opposed to NASA's large summer values. In fact, nearly all urban KNMI averages were largest in cooler months. This is matched to a smaller degree in the AIRPACT results and suggests that NO_2 levels near urban areas are higher in winter than in summer. The cause for this winter/summer difference is probably a complex balance between less photolysis of NO_2 in winter associated with lower sun angles and greater photochemical processing of NO_x to HNO_3 in summer.

3.4 Effects of applying the averaging kernel

In order to decrease the number of comparison errors, for reasons given above, it is appropriate to apply the averaging kernel to AIRPACT results for the best numerical comparison between AIRPACT and OMI. The programs and GEOS-CHEM lookup tables provided by Bucsela (private communication) allowed us to calculate averaging kernels from AMFs derived in the NASA algorithms. Note that these kernels are not official NASA averaging kernels and so represent a research grade dataset. NASA does not publicly provide averaging kernels to the users currently, but KNMI did start providing them in 2008, when there was a data format upgrade. We have computed the monthly average column abundances of AIRPACT for July 2007, and January 2008, using the averaging kernels, to determine the significance of the modified columns.

A comparison of OMI tropospheric NO_2 averaging kernel profiles for Seattle, are shown in Fig. 13 for July 2007 and January 2008. The KNMI averaging kernels do not extend as far up into the atmosphere as the NASA averaging kernels because the coding provided to calculate NASA averaging kernels allowed us the flexibility to apply an averaging kernel to the entire AIRPACT profile. This is in contrast to the KNMI averaging kernels, which are calculated by the user with variables provided in the daily product, and use a predefined top pressure layer. Furthermore, NASA a priori profiles and averaging kernels extend to 1020 hpa for all pixels, regardless of terrain height. This is due to the method used to integrate columns in the OMI NO_2 product, where the profile is truncated at the surface pressure for each pixel. This is in contrast to the KNMI a priori profiles and averaging kernels,

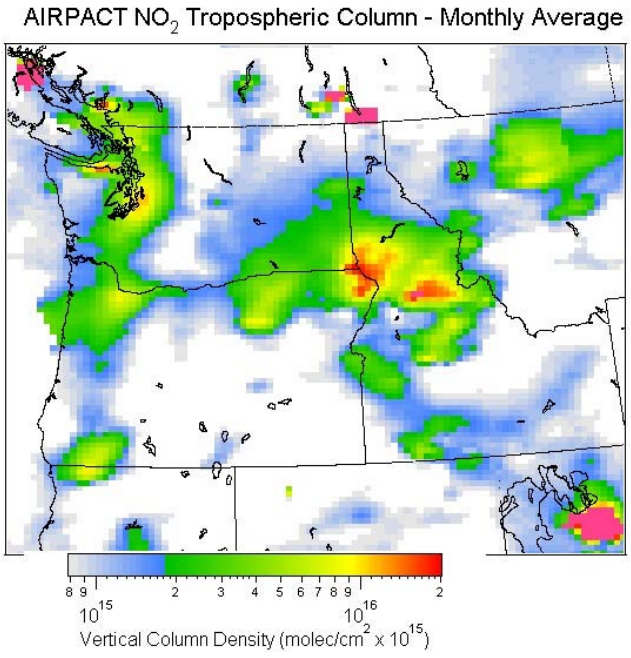

Fig. 15. AIRPACT tropospheric NO_2 column with the daily averaging kernels from OMI applied to AIRPACT are shown for a summer (July 2007) monthly average: AIRPACT × NASA AK using the code provided by Bucsela using an integration method similar to the OMI data product. This integration technique is a function of pressure per layer but not temperature or layer thickness. Compared to the upper right panel of Fig. 14, this method decreases the background bias but also leads to erroneously large values at times (shown as pink).

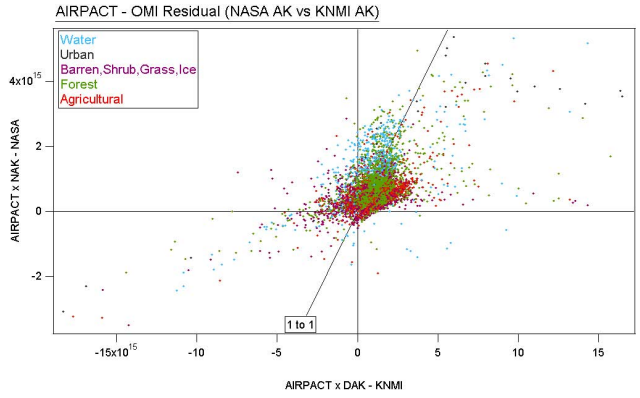

Fig. 16. AIRPACT – OMI tropospheric NO_2 column residuals with the daily averaging kernels from OMI applied to AIRPACT is shown for a winter (January 2008) monthly average. This scatter plot of AIRPACT × NASA AK – NASA OMI vs AIRPACT × DAK – KNMI OMI is separated by color into dominant land class type (obtained from the US National Land Class Database and GEOBASE Canada, 2001 Land Class/Land Use using LandSat-7 derived radiances survey). One would expect the distribution to fall along the 1 to 1 line if the two products suggested the same model biases.

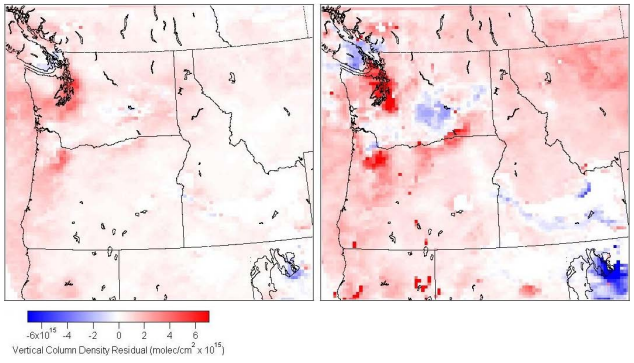

Fig. 17. AIRPACT – OMI tropospheric NO_2 column residuals with the daily averaging kernels from OMI applied to AIRPACT is shown for a winter (January 2008) monthly average. AIRPACT × NASA AK - NASA OMI is shown on left while AIRPACT × DAK – KNMI OMI is shown on the right. Some values are over 6 × 10^{15} molecules per square centimeter as shown in Fig. 16. Note the large positive bias found in discrete pixels in the right panel, indicative of extreme negatives in the KNMI data product dominating the monthly average of an unpolluted area, apparently due to the stratospheric subtraction methods used.

which only extend down to approximately the surface. Another difference between the two averaging kernel profiles is that the NASA kernel seems to reflect a step function while the KNMI kernel is more linear. We can also clearly see that the KNMI kernels are higher in the winter, compared to the summer, across the entire vector. NASA kernels, on the other hand, are less in the upper troposphere and more in the lower troposphere in the winter, compared to summer. Overall, the magnitude of the NASA kernel is much larger than the KNMI kernel in the summer, but they are relatively close in the winter.

The results of applying the averaging kernels to the AIRPACT columns are shown for July 2007 and January 2008 in Fig. 14. The most notable change is in summer when applying the NASA averaging kernel, where there is a blanket increase across the entire domain as a direct response to the high averaging kernel values computed. This does not occur in the winter. The integration technique used in our standard methods calculates number density using pressure, layer thickness, and temperature. However, an alternative method that is only dependent on pressure is available in the code that Bucsela provided with an integration technique similar to the NASA algorithms. When using this method in the summer, the background increase does not occur across the domain, but erroneously large values appear in areas that otherwise had no significant NO_2 concentrations, as shown in Fig. 15. These values tend to be over 1×10^{17} molecules per square centimeter and occur when the integration technique used overcompensates for successive layers that are numerically similar. The numerical results of the code are less reliable for computing monthly averages because of the erroneously

Table 4. Differences in average tropospheric NO_2 for urban areas as a result of applying the averaging kernels from KNMI and NASA. Summer (July 2007) and winter (January 2008) monthly averages are shown. KNMI and NASA columns are provided as well for reference.

JULY 2007 – Urban Area Tropospheric Column NO_2*							
* All values are in molecules per square centimeter $\times 10^{15}$							
	AIRPACT	AIRPxAK (KNMI)	% Change due to AK	KNMI	AIRPxAK (NASA)	% Change due to AK	NASA
Seattle	7.5	4.9	*−34.7%*	4.4	11.8	*57.3%*	7.0
Boise	2.4	1.3	*−45.8%*	1.5	3.5	*45.8%*	2.8
Portland	4.7	2.5	*−46.8%*	3.2	8.2	*74.5%*	6.3
Salt Lake City	4.9	2.7	*−44.9%*	5.3	5.9	*20.4%*	4.2
Vancouver, BC	3.0	1.5	*−50.0%*	4.9	5.7	*90.0%*	7.4
JANUARY 2008 – Urban Area Tropospheric Column NO_2*							
* All values are in molecules per square centimeter $\times 10^{15}$							
	AIRPACT	AIRPxAK (KNMI)	% Change due to AK	KNMI	AIRPxAK (NASA)	% Change due to AK	NASA
Seattle	8.9	11.5	*29.2%*	7.3	9.2	*3.4%*	4.9
Boise	2.9	2.3	*−20.7%*	2.7	2.7	*−6.9%*	2.3
Portland	4.5	5.4	*20.0%*	4.5	6.3	*40.0%*	5.1
Salt Lake City	8.4	13.9	*65.5%*	25.2	7.6	*−9.5%*	6.8
Vancouver, BC	5.6	6.0	*7.1%*	9.2	6.3	12.5%	6.3

large values. However, it does add another useful perspective when comparing AIRPACT's summer months to the NASA product. Also, note that new code has recently been developed by Bucsela that may fix some of these issues.

The differences in AIRPACT's average tropospheric NO_2 for urban areas as a result of applying the averaging kernels from KNMI and NASA for summer (July 2007) and winter (January 2008) monthly averages are shown in Table 4. Figures 16 and 17 show the distribution and maps of AIRPACT – OMI tropospheric NO_2 column residuals with the daily averaging kernels applied to AIRPACT for both KNMI and NASA. From this comparison we conclude that AIRPACT overestimates NO_2 in the areas around Portland and Seattle but underestimates it in Salt Lake City.

4 Conclusions

In our 18-month analysis of tropospheric NO_2 in the Pacific Northwest, we found a number of significant findings in both the OMI data and the relationship to regional forecasts by AIRPACT. There is a seasonal pattern of OMI tropospheric NO_2 from NASA, where high values are reported in the summer and low values in the winter, presumably a systematic outcome due to assumptions in the NASA algorithms and the seasonal variations in stratospheric NO_2. Despite this problem, we can clearly see that AIRPACT underestimates emissions in Canadian urban areas and sometimes overestimates in some USA urban areas. This may be due to discrepancies in the way that emissions inventories are calculated in these two countries. Applying the OMI averaging kernels to the model results gives a comparison with the least possible introduced error, but the differences between the NASA and KNMI are large enough to warrant concern about the accuracy of OMI tropospheric NO_2 products, especially in areas of complex terrain and low pollution. This difference makes it difficult for users to decide which data set to use for comparison. However, the KNMI product includes the averaging kernel and the NASA product shows a clear systematic seasonal cycle, which makes the KNMI product more desirable despite the inclusion of negative values.

Although there are sources of error in the OMI retrieval of NO_2, and limiting factors such as cloud cover, OMI provides a good source of data for evaluating a CTM, including larger errors in emissions, over a long term period. Computing monthly averages of NO_2 in relatively cloud free conditions provided a significant database for evaluating the AIRPACT NO_x forecast levels. There are minor problems when comparing tropospheric NO_2 columns, such as stratospheric NO_2 abundances and a priori assumptions. However, long term results for biases between OMI and a CTM gives researchers a means to evaluate modeled NO_x in the troposphere for an entire modeling domain. This is a valuable source of validation in areas with a limited number of ground based NO_x monitors, as is the case in the Pacific Northwest.

There are important implications for modeled ozone performance given the biases found using the OMI products. The urban areas in the domain are consistently VOC limited and so we would expect predicted ozone in Seattle to increase after a downward NO_x emissions correction. AIRPACT predictions of summer wild fire emissions were found to be too frequent, with burning in the same locations occurring over too long a period. We look forward to working with the new BlueSky framework for processing wildfire emissions which should help to minimize error in wildfire locations and radiant energy.

Acknowledgements. This research was made possible by a grant from NASA for the North-West-AIRQUEST Decision Support System (grant #NNA06CN04A). The authors would like to thank Eric Bucsela as well as OMI team members from KNMI and NASA for their support in this project.

Edited by: R. Cohen

References

Blond, N., Boersma, K. F., Eskes, H. J., van der A, R. J., Roozendael, M. V., Smedt, I. D., Bergametti, G., and Vautard, R.: Intercomparison of SCIAMACHY nitrogen dioxide observations, in situ measurements and air quality modeling results over Western Europe, J. Geophys. Res., 112, D10311, doi:10.1029/2006JD007277, 2007.

Boersma, K .F., Dirksen, R. J., Veefkind, J. P., Eskes, H. J., and van der A, R. J.: Dutch OMI NO2 (DOMINO) data product, HE5 data file user manual. Tropospheric Emission Monitoring Internet Service (TEMIS), Royal Netherlands Meteorological Institute (KNMI), available at: http://www.temis.nl/docs/OMI_NO2_HE5_1.01_29042008.pdf, April 2008.

Boersma, K. F., Eskes, H. J., and Brinksma, E. J.: Error Analysis for tropospheric NO_2 retrieval from space, J. Geophys. Res., 109, D04311, doi:10.1029/2003JD003962, 2004.

Boersma, K. F., Eskes, H. J., Veefkind, J. P., Brinksma, E. J., van der A, R. J., Sneep, M., van den Oord, G. H. J., Levelt, P. F., Stammes, P., Gleason, J. F., and Bucsela, E. J.: Near-real time retrieval of tropospheric NO_2 from OMI, Atmos. Chem. Phys., 7, 2103–2118, doi:10.5194/acp-7-2103-2007, 2007.

Boersma, K. F., Jacob, D. J., Bucsela, E. J., Perring, A. E., Dirksen, R., van der A, R. J., Yantosca, R. M., Park, R. J., Wenig, M. O., Bertram, T. H., and Cohen, R. C.: Validation of OMI tropospheric NO2 observations during INTEX-B and application to constrain NO_x emissions over the eastern United States and Mexico, Atmos. Environ., 42, 4480–4497, 2008.

Boersma, K. F., Dirksen, R. J., Veefkind, J. P., Eskes, H. J., and van der A, R. J.: Dutch OMI NO_2 (DOMINO) data product, HE5 data file user manual, available at: http://www.temis.nl/docs/OMI_NO2_HE5_1.0.2.pdf, April 2009.

Bucsela, E. J., Celarier, E. A., Wenig, M. O., Gleason, J. F., Veefkind, J. P., Boersma, K. F., and Brinksma, E. J.: Algorithm for NO_2 vertical column retrieval from the ozone monitoring instrument, IEEE T. Geosci. Remote, 44(4), 1245–1258, doi:10.1109/TGRS.2005.863715, 2006.

Bucsela, E. J., Perring, A. E., Cohen, R. C., et al.: Comparison of tropospheric NO_2 from in situ aircraft measurements with near-real-time and standard product data from OMI, J. Geophys. Res., 113, D16S31, doi:10.1029/2007JD008838, 2008.

Byun, D. and Schere, K. L.: Review of the Governing Equations, Computational Algorithms, and other components of the models-3 community multiscale air quality (CMAQ) modeling system, Appl. Mech. Rev., 59(51), doi:10.1115/1.2128636, 2006.

Celarier, E. A. and Retscher, C.: OMNO2e Data Product Readme File, Document Revision 1.2, NASA Goddard Space Flight Center, available at: http://toms.gsfc.nasa.gov/omi/no2/OMNO2e_DP_Readme.pdf, November 2009.

Celarier, E. A., Brinksma, E., Gleason, J. F., Veefkind, J. P., Cede, A., Herman, J. R., Ionov, D., Goutail, F., Pommereau, J., Lambert, J., Van Roozendael, M., Pinardi, G., Wittrock, F., Schonhardt, A., Richter, A., Ibrahim, O. W., Wagner, T., Bojkov, B. R., Mount, G. H., Spinei, E., Chen, C., Pongetti, T., Sander, S. P., Bucsela, E., Wenig, M., Swart, D., Volten, H., Kroon, M., and Levelt, P.: Validation of Ozone Monitoring Instrument Nitrogen Dioxide Columns, J. Geophys. Res., 113, D15S15, doi:10.1029/2007JD008908, 2008.

Chance, K.: OMI Algorithm Theoretical Basis Document, Vol. 4, OMI Trace Gas Algorithms, Smithsonian Astrophysical Observatory, available at: http://eospso.gsfc.nasa.gov/eos_homepage/for_scientists/atbd/docs/OMI/ATBD-OMI-04.pdf, 2002.

Chen, J., Vaughan, J., Avise, J., O'Neill, S., and Lamb, B.: Enhancement and evaluation of the AIRPACT ozone and $PM_{2.5}$ forecast system for the Pacific Northwest, J. Geophys. Res., 113, D14305, doi:10.1029/2007JD009554, 2008.

Cohen, C. and Murphy, J.: Photochemistry of NO2 in Earth's stratosphere: constraints from observations, American Chemical Society, Chem. Rev., 103(12), 4985–4998, doi:10.1021/cr020647x, 2003.

Dirksen, R., Eskes, H., Boersma, F., Levelt, P., Veefkind, P., and van der A, R.: Derivation of Ozone Monitoring Instrument tropospheric NO_2 in near real time (DOMINO); Final Report, Netherlands Agency for Aerospace Programmes, available at: http://www.knmi.nl/~eskes/projects/DOMINO_final_report_april2008.pdf, 2008.

Elbern, H., Strunk, A., Schmidt, H., and Talagrand, O.: Emission rate and chemical state estimation by 4-dimensional variational inversion, Atmos. Chem. Phys., 7, 3749–3769, doi:10.5194/acp-7-3749-2007, 2007.

EPA: User's Guide to MOBILE 6.1 and 6.2: Mobile Source Emission Factor Model, EPA420-R-03-010, US Environmental Protection Agency, August 2003.

Eskes, H. J. and Boersma, K. F.: Averaging kernels for DOAS total-column satellite retrievals, Atmos. Chem. Phys., 3, 1285–1291, doi:10.5194/acp-3-1285-2003, 2003.

Kaynak, B., Hu, Y., Martin, R. V., Sioris, C. E., and Russell, A. G.: Comparison of weekly cycle of NO_2 satellite retrievals and NO_x emission inventories for the continental United States, J. Geophys. Res., 114, D05302, doi:10.1029/2008JD010714, 2009.

Kim, S.-W., Heckel, A., Frost, G. J., Richter, A., Gleason, J., Burrows, J. P., McKeen, S., Hsie, E.-Y., Granier, C., and Trainer, M.: NO_2 columns in the western United States observed from space and simulated by a regional chemistry model and their implications for NO_x emissions, J. Geophys. Res., 114, D11301, doi:10.1029/2008JD011343, 2009.

Kramer, L. J., Leigh, R. J., Remedios, J. J., and Monks, P. S.: Comparison of OMI and ground-based in situ and MAX-DOAS measurements of tropospheric nitrogen dioxide in an urban area, J. Geophys. Res., 113, D16S39, doi:10.1029/2007JD009168, 2008.

Kurokawa, J., Yumimoto, K., Uno, I., and Ohara, T.: Adjoint inverse modeling of NO_x emissions over eastern China using satellite observations of NO_2 vertical column densities, Atmos. Environ., 43, 1878–1887, 2009.

Mass, C. F., Albright, M., Ovens, D., Steed, R., MacIver, M., Grimit, E., Eckel, T., Lamb, B., Vaughan, J., Westrick, K., Storck, P., Colman, B., Hill, C., Maykut, N., Gilroy, M., Ferguson, S. A., Yetter, J., Sierchio, J. M., Bowman, C., Stender, R., Wilson, R., and Brown, W.: Regional Environmental Prediction over the Pacific Northwest, B. Am. Meteorol. Soc., 84, 1353–1366, 2003.

Mijling, B. and van der A, R.: Product Specification Document: Long Range Transport of Tropospheric NO_2 observed by the OMI instrument, TEMIS, available at: http://www.temis.nl/docs/PSD_NO2_LRT.pdf, 2007.

Mijling, B., van der A, R. J., Boersma, K. F., Van Roozendael, M., De Smedt, I., and Kelder, H. M.: Reductions of NO_2 detected from space during the 2008 Beijing Olympic Games, J. Geophys. Res., 36, L13801, doi:10.1029/2009GL038943, 2009.

Napelenok, S. L., Pinder, R. W., Gilliland, A. B., and Martin, R. V.: A method for evaluating spatially-resolved NO_x emissions using Kalman filter inversion, direct sensitivities, and space-based NO_2 observations, Atmos. Chem. Phys., 8, 5603–5614, doi:10.5194/acp-8-5603-2008, 2008.

OMNO2 README File, available at: http://toms.gsfc.nasa.gov/omi/no2/OMNO2_readme.pdf, 2009.

Parrish, D.: Critical Evaluation of US on-road vehicle emission inventories, Atmos. Environ., 40, 2288–2300, 2006.

Pollack, A. K., Lindhjem C., Stoeckenius, T. E., Tran, C., Mansell, G., Jimenez, M., Wilson, G., and Coulter-Burke, S.: Evaluation of the U.S. EPA MOBILE6 Highway Vehicle Emission Factor Model, ENVIRON International Corporation, www.epa.gov/OMS/models/mobile6/crce64.pdf, 2004.

Schaub, D., Boersma, K. F., Kaiser, J. W., Weiss, A. K., Folini, D., Eskes, H. J., and Buchmann, B.: Comparison of GOME tropospheric NO_2 columns with NO2 profiles deduced from ground-based in situ measurements, Atmos. Chem. Phys., 6, 3211–3229, doi:10.5194/acp-6-3211-2006, 2006.

Tang, T., Roberts, M., and Ho, C.: Sensitivity Analysis of MOBILE6 Motor Vehicle Emission Factor Model, US Department of Transportation, Federal Highway Administration, available at: http://www.fhwa.dot.gov/resourcecenter/teams/airquality/mobile6_v2.pdf, 2002.

Zhao, C. and Wang, Y.: Assimilated inversion of NO_x emissions over east Asia using OMI NO_2 column measurements, Geophys. Res. Lett., 36, L06805, doi:10.1029/2008GL037123, 2009.

Zubrow, A., Chen, L., and Kotamarthi, V. R.: EAKF-CMAQ: Introduction and evaluation of a data assimilation for CMAQ based on the ensemble adjustment Kalman filter, J. Geophys. Res., 113, D09302, doi:10.1029/2007JD009267, 2008.